Coarse-to-fine Grained Image Splicing Localization Method Based on Noise Level Inconsistency

Xiaofeng Wang, Qian Zhang, Chuntao Jiang, Ying Zhang

Abstract-Image splicing detection is one of the important technologies to protect image content authenticity. In this work, we propose a coarse-to-fine grained image splicing localization method. The proposed method is based on the fact is that the noise level of the splicing image region is inconsistent with that of the original image region. In the proposed method, we used Laplace operator to extract the local noise of the image, and estimated the local correlation feature by using the prediction residual. Then, we use the clustering algorithm for coarse grained splicing localization to get suspicious spliced regions, and use an approach of connected region expansion/corrosion for fine grained detection to get the precise splicing regions. Compared with the existing noise-based image splicing localization methods, the proposed method has high detection accuracy and stronger robustness to content-preserving manipulations.

***Keywords*-Image splicing detection, SLIC, Noise level estimation, Coarse-to-fine grained splicing localization**

I. INTRODUCTION

With the rapid development of the digital image processing technology, the application of large-scale image/video database has become ubiquitous. At the same time, the emergence of many powerful and easy-to-control image processing software such as Adobe Photoshop, MeiTu, make it is easy for non-professional users to manipulate and modify image content. In recent years, a variety of photo forgery incidents occurred frequently. The existence of fake images seriously reduces the credibility of image information, and has caused serious negative effects in many fields such as scientific research, news media, political events, medical diagnosis, cultural media, evidence falsification, finance, and military and so on. Therefore, digital image tampering detection technology has become a hot research topic in recent years, and it has important theoretical significance and practical application value.

Digital image forensics is one of the main technologies for image content authenticity protection. It includes active forensics [1-3] and passive (blind) forensics [4-6]. Due to the prior information cannot be obtained in practical application, passive forensics methods are more practical. Therefore, in recent years, image passive forensics methods have received great attention. Passive forensics mainly includes image tampering detection, image source identification and operation history tracking. As image splicing/compositing is a common image tampering approach, in this paper, we devote ourselves to research the method of image splicing tampering detection. Image splicing refers to the copying and pasting of a part of image content into another image with the purpose of tampering image content and forging non-existent scenes.

A. Prior Works

In recent years, image splicing detection methods have been widely studied. Among the existing literature, the methods of image splicing detection can be roughly divided into two categories: image splicing detection and splicing regions detection. The former detects whether the image is a composite image [7], and the latter detect and seek the splicing regions in the image.

Most of the early methods are splicing detection approaches. These methods are actually image classification methods that classify spliced image from natural images. In recent years, image splicing regions detection and localization technologies have attracted widespread attention. According to the difference of extracted forensics features, methods in existing literature can be roughly divided into the following main types: Photo Response Non-Uniformity (PRNU) noise based methods [8], the inconsistency of Color filter array (CFA) based methods [9], double (multiple) JPEG compression detection methods [10], and blur inconsistencies based detection methods [11], etc.

Due to different images have different noise levels, in a composite image, the noise levels of the splicing regions is inconsistent with the noise levels of whole image. This inconsistency can be used as evidence of image splicing forensics. In [12], the author used a median-filtering-based noise estimator [13] to estimate the noise variance in each image block, and used inconsistencies of local noise levels to locate the splicing regions. The disadvantage of this method is that the threshold value must be carefully selected; otherwise it is difficult to separate the splicing regions from the image. In [14], the authors used a noise variance estimation method based on PCA to estimate the noise variance of regular image blocks, and then used the K-means clustering algorithm to cluster the noise variance, and finally obtained the splicing regions. However, this method ignores the influence of noise variance estimation on image content, so it has high false detection. The work [15] proposed a method based on noise parameter inconsistency. According to the camera and lighting conditions during the process of image acquisition, this method use the fact that different images have different noise characteristics, and separates the splicing regions from the image by highlighting the local noise inconsistency in the quadtree scan of the image. The work [16] proposed an image splicing forgery detection method based on multi-scale noise estimation. In this method, the author first used the super pixel segmentation algorithm to segment the image into multi-scale super pixels, and then calculated the noise level function that reflects the relationship between the noise level and the brightness of each super pixel in each individual scale. Super pixel blocks which are not constrained by noise level function are considered as the suspicious splicing regions.

978-1-7281-4905-9/20/$31.00 ©2020 IEEE

B. Our Contributions

In this work, we propose a method of image splicing regions detection using a coarse-to-fine grained splicing localization strategy. In the proposed method, we propose a two phases image splicing localization algorithm. In the proposed method, we extract the local noise of the image and estimate the local correlation features by using the predicted residuals, then we detect the splicing image regions from coarse grained to fine grained. Finally, more accurate splicing regions can be detected. Furthermore, The OTSU method is used to generate system parameters, rather than experimental results or man-made setting. The proposed method is provided with strong robustness for various content-preserving manipulations.

II. The Proposed Method

A. Feature Extraction

1) The Image Block Division

Using the SLIC [17], the image I with size $M \times N$ is divided into K non-overlapping super pixel blocks. Since the super pixel blocks are irregular image blocks, to extract Laplace noise for each image blocks, we extend each super pixel block to form a regular rectangular region. The extend rules are as follows:

For the irregular super pixel block K_i, the maximum row/column labels and the minimum row/column labels are denoted as $\max\_m$, $\max\_n$, $\min\_m$ and $\min\_n$, respectively. Let $B_i(i=1,2,\cdots,K)$ denoted the circumscribed rectangular area enclosed by these four labels. Then B_i is a regular expending block of the super-pixel block K_i.

2) Laplace Noise Features

In composite image, the splicing operation will introduce additional splicing edges, which are sharper than the original information in natural image. We can think the splicing edges as a special noise introduced by splicing operation. Considering that the Laplace operator has good edge detection functionality, we use Laplace operator to estimate the local noise of image blocks. Laplace noise estimation operator is a mask operation algorithm used for image processing and analysis. According to literature [18], it can be represented as follows:

$$L = 2 \times (L_2 - L_1) = \begin{pmatrix} 1 & -2 & 1 \\ -2 & 4 & -2 \\ 1 & -2 & 1 \end{pmatrix} \tag{1}$$

Where, $L_1 = \begin{pmatrix} 0 & 1 & 0 \\ 1 & -4 & 1 \\ 0 & 1 & 0 \end{pmatrix}$ and $L_2 = \frac{1}{2} \times \begin{pmatrix} 1 & 0 & 1 \\ 0 & -4 & 0 \\ 1 & 0 & 1 \end{pmatrix}$.

Then, the noise standard deviation $\sigma_i(i=1,2,...,K)$ of the image block S_i can be calculated as follows:

$$\sigma_i = \sqrt{\frac{\pi}{2}} \frac{1}{6(M-2)(N-2)} \sum |V_i| \tag{2}$$

Let M_{B_i} represents the matrix of image block B_i. Where, M and N are the width and height of the image I, $i=1,2,\cdots,K$. Let $V_i = M_{B_i} * L$, here, * represents the convolution operation. $\sum |V_i|$ represents the sum of the absolute values of the elements in matrix V_i.

Local Laplace noise features are defined as:

$$\varpi = (\sigma_1, \sigma_2, \cdots, \sigma_K) \tag{3}$$

3) Local Correlation Features

In natural image, there is strong correlation between adjacent pixels. In splicing image, the operation of image splicing will introduce additional splicing edges, and these splicing edges will destroy the correlation of pixels in natural images. This property can be used as a clue to detect splicing image regions. In order to detect the spliced image regions, we calculate the predicted image I' of image I, then subtract the predicted image I' from the image I to obtain the predicted error image ΔI. Prediction error image reduces the impact caused by the diversity of image content, and meanwhile enhances the information introduced by image splicing operation.

Let

$$\Delta I = I - I' \tag{4}$$

According to literature [19], the predicted pixel value p' can be expressed by the formula (5):

$$p' = \begin{cases} \max(a,b), c \le \min(a,b) \\ \min(a,b), c \ge \max(a,b) \\ a+b-c, otherwise \end{cases} \tag{5}$$

Where, a,b,c are the adjacent pixels of pixel p. The location of a,b,c is shown in Fig.1.

p	a
b	c

Fig.1. Context prediction

For image I and predicted image I', we perform the super pixel segmentation, respectively, and then the super pixel blocks are extended into regular blocks respectively, which are denoted as:

$BI = (B_1, B_2, \cdots, B_K)$, and $BI' = (B_1', B_2', \cdots, B_K')$.

To investigate the correlation between image blocks B_i and B_i', we estimate the Person correlation coefficient $r_i(i=1,2,...,K)$ as follows:

$$r_i = \frac{\sum_{j=1}^{n} (b_j - \overline{b})(b_j' - \overline{b'})}{\sqrt{\sum_{j=1}^{n} (b_j - \overline{b})^2 \sum_{j=1}^{n} (b_j' - \overline{b'})^2}} \tag{6}$$

Where, $B_i = (b_1, b_2, ..., b_n)$, $B_i' = (b_1', b_2', ..., b_n')(i=1,2,\cdots,K)$, $b_j(j=1,2,...,n)$ and $b_j'(j=1,2,...,n)$ are the pixel values in the extended blocks B_i and B_i', respectively, and n is the number of pixels in the block.

Then the local correlation features are defined as:

$$R = (r_1, r_2, \cdots, r_K) \tag{7}$$

B. Tampering Region Localization

1) Coarse-Grained Tampering Region Localization

Fuzzy C-means (FCM) clustering [20] is an effective method of data analyzing and modeling. It has been used in various fields such as large-scale data analysis, data mining, image segmentation, pattern recognition, and so on. In a splicing image, we believe that the image contents can be divided into two parts, splicing regions and non-splicing regions.

We use the FCM clustering algorithm to cluster the Laplace noise standard deviation $\sigma_i(i=1,2,...,K)$ into two categories: A_1 and A_2.

Let

$$c_1 = \underset{B_i \subseteq A_1}{count}(B_i),\ c_2 = \underset{B_i \subseteq A_2}{count}(B_i) \tag{8}$$

where $count(\cdot)$ is a counting function, it returns the number of image blocks in each category.

In general, we think that the spliced image regions should occupy smaller areas of the image, so we regard the image block contained in a few classes as the spliced regions. Then the splicing region is defined as:

$$A' = \begin{cases} A_1, c_2 > c_1 \\ A_2, otherwise \end{cases} \tag{9}$$

If $r_i > \tau_1$ and $B_i \in A'$, then the i^{th} super pixel block is considered as a suspicious splicing block. Let Q denote the set of suspicious super pixel blocks. Where, τ_1 is the preset threshold.

2) Fine-Grained Tampering Region Localization

(1) Region Expansion

In order to obtain more accurate tampering detection results, we conducted fine-grained detection on the obtained suspicious splicing block set Q. In general, a splicing region in the splicing image is a connected region. Therefore, we first seek the largest connected region in set Q, denoted as P.

Search the maximum row/column labels and minimum row/column labels of the connected region P, denoted as $\max\_mp$, $\max\_np$, $\min\_mp$ and $\min\_np$, respectively. To improve the detection accuracy, we expand the region P, and the expanded row/column labels can be expressed as follows:

$$h_1 = \begin{cases} \min\_mp - k_1, if\ \min\_mp - k_1 > 0 \\ 1, otherwise \end{cases} \tag{10}$$

$$h_2 = \begin{cases} \max\_mp + k_1, if\ \max\_mp + k_1 < M \\ M, otherwise \end{cases} \tag{11}$$

$$l_1 = \begin{cases} \min\_np - k_2, if\ \min\_np - k_2 > 0 \\ 1, otherwise \end{cases} \tag{12}$$

$$l_2 = \begin{cases} \max\_np + k_2, if\ \max\_np + k_2 < N \\ N, otherwise \end{cases} \tag{13}$$

Where, $k_1 = round(M/32)$, $k_2 = round(N/32)$, and $round(\cdot)$ means round down.

The size of the sub-block should be moderate, if the sub-block is too large, the tampered regions cannot be accurately located. If the sub-block is too small, the information content in the block is not sufficient, and more false checks are likely to occur, and the operation time is too long. According to the experimental comparison, the sub-block with a size of 16×16 is selected in this paper. Fig.2 shows the visual effect of the detection results with different size of blocks, as can be seen from the Fig.2, when the size of the image block is 16×16, the detection accuracy was relatively high.

(64×64) (32×32) (16×16) (8×8)

Fig.2. Different block localization results

Let Ω represent the rectangular region enclosed by the four newly obtained labels h_1, h_2, l_1, l_2, as shown in Fig.3. In the Fig.3(a), the region P is marked by blocks with red digital labels. In the Fig.3(b), the red rectangular region is the region Ω that is generated via expanding the region P. Then the region Ω is divided into non-overlapping 16×16 regular blocks. We calculate the Laplace noise of each block:

$$n' = (n'_1, n'_2, \cdots, n'_l) \tag{14}$$

Where, $l = ((\max\_mp - \min\_mp) \times (\max\_np - \min\_np))/16 \times 16$, τ_2 is the threshold. If $n'_q > \tau_2 (q = 1,2,\cdots,l)$, the q^{th} block is considered to be a suspicious splicing block.

a b

Fig.3. Circumscribed rectangular region

(2) Connected Region Expansion/Corrosion

In order to reduce the detection errors, we use an approach of connected region expansion/corrosion for fine grained detection. Now we describe its operating principle.

If an image block B is detected as a splicing block, but all its adjacent image blocks are detected as real blocks, then the block B should be removed from the set of suspicious splicing blocks, as shown in Fig.4(a). On the contrary, if an image block B is detected as a real block, and all its adjacent image blocks are detected as suspicious blocks, then the block B should be added into the set of suspicious splicing blocks, as shown in Fig.4(b). Using connected region expansion/corrosion, the final set of splicing blocks can be obtained, and the splicing regions can be detected.

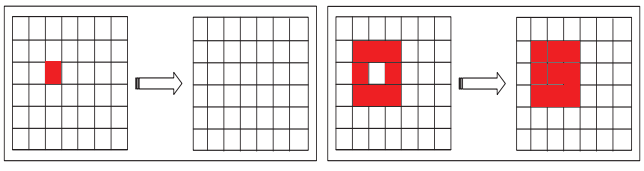

(a) (b)

Fig.4. Connected region expansion/corrosion

III. Experimental Results and Performance Analysis

In this section, we evaluate the proposed solution via simulation experiment. We implemented and tested our method using MATLAB R2014a. The experiment was run on a computer with an Intel(R) Core(TM) CPU, i5-3470 @ 3.2GHz, 4.00GB RAM.

A. Parameters Evaluation for Adaptive Threshold

We use the OTSU method to determine the tampering localization thresholds τ_1 and τ_2. The OTSU method is also known as the maximum inter-class variance method. It is an adaptive threshold determination algorithm proposed by Nobuyuki Otsu in 1979 [21]. The OTSU algorithm uses the idea of clustering, it divides the pixels into two class according to estimate an appropriate variance of the pixels that make the difference of inter-class is largest, and the difference of inter-class is smallest. Therefore, for the two-classification problems, the OTSU algorithm can be used to automatically select threshold value that divide the data into two parts. The algorithm process is as follows.

To estimate the threshold value τ_1, we investigate the Person correlation coefficient between the tested image I and the predicted image $I^{'}$ corresponding to the extended rule blocks.

Our goal is seeking for a value $\alpha_s \in R$ that divide set R into two sub-sets W_1 and W_2, such that the difference between W_1 and W_2 is maximum, and the differences within W_1 and W_2 are minimum. Assuming W_1 and W_2 can be denoted as $W_1 = (r_{\alpha_1}, r_{\alpha_2}, ..., r_{\alpha_s})$, $W_2 = (r_{\alpha_{s+1}}, r_{\alpha_{s+2}}, ..., r_K)$, then the probability of W_1 and W_2 is:

$$e_1 = \|W_1\| / K \tag{15}$$

$$e_2 = 1 - \|W_1\| / K \tag{16}$$

Where $\|\cdot\|$ represents the cardinality of the set.

Then, the mean values of W_1 and W_2 are:

$$m_1 = \frac{1}{\|W_1\|} \sum_{i=\alpha_1}^{\alpha_s} r_i \tag{17}$$

$$m_2 = \frac{1}{K - \|W_1\|} \sum_{i=\alpha_{s+1}}^{K} r_i \tag{18}$$

Let $m_{total} = e_1 m_1 + e_2 m_2$. The variance between W_1 and W_2 is:

$$v^2(\alpha_s) = e_1 (m_1 - m_{total})^2 + e_2 (m_2 - m_{total})^2 \tag{19}$$

Our goal is seeking for a value $\alpha_s^* \in R$ such that

$$\alpha_s^* = Arg \max_{\alpha_s} [v^2(\alpha_s)] \tag{20}$$

Then α_s^* is the required threshold value τ_1. Similarly, we can get the threshold τ_2.

B. Visual Effects of Splicing Region Detection

To demonstrate the effectiveness of the proposed method, we use the proposed method to test splicing images that come from Columbia IPDED image library [23], and manually spliced images that come from the BSDS200 database. The tampering localization results are shown in the Fig.5.

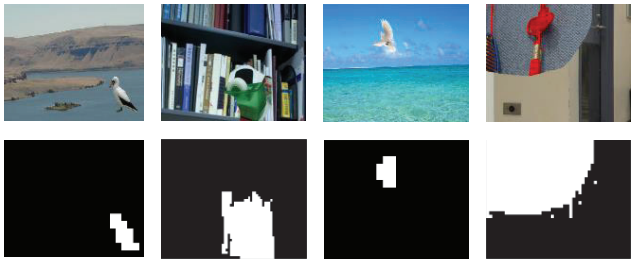

Fig.5. Visual results of splicing detection

In order to illustrate the advantage of the proposed method, we compare the visual effect with that of literature [22] and [14]. In the experiment, the tested images come from Columbia IPDED image library, and an uncompressed public database [23]. Fig.6 shows some examples of tested images and their detection results. In Fig.6, the first line represents the tested images, the second line represents the detection results of the proposed method, the third line represents the detection results of literature [22], and the fourth line represents the detection results of literature [14]. The white regions in the detection results represent the detected splicing regions, and the black regions represent the original image regions.

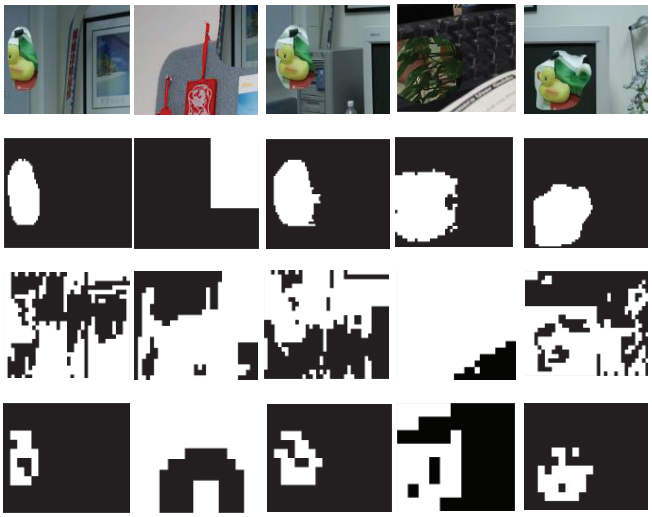

(a) (b) (c) (d) (e)

Fig.6. Splicing detection results and comparison

To quantitatively evaluate the detection performance of the proposed method, we use true positive rate (TPR) and false positive rate (FPR) as the measurement criteria:

$$TPR = \frac{TP}{TP + FN} \qquad \text{and} \qquad FPR = \frac{FP}{FP + TN}$$

Where, TP represents the number of pixels are correctly detected in the tampering regions, FN represents the number of pixels that are in the tampering regions but are not detected, and FP represents the number of pixels are incorrectly detected in the tampering regions. TPR refers to the ratio that the splicing pixels are detected as splicing pixels; FPR is the ratio that real pixels are detected as the splicing pixels.

We calculated the pixel level TPR and FPR of the detection results in Fig.6, and the results are shown in Table 1.

Table 1 The pixel level detection accuracy

		The proposed method	[22]	[14]
(a)	TPR	99.9	62.4	67.8
	FPR	1.4	55.4	0.51
(b)	TPR	100	99.3	94.6
	FPR	10.8	56.2	65.7
(c)	TPR	100	75.1	67.3
	FPR	5.4	47.8	1.59
(d)	TPR	91.2	100	82.1
	FPR	2.1	84.7	18.9
(e)	TPR	99.9	62.5	65.2
	FPR	2.8	47.6	0.93

According to the results in Table 1, we can see that the detection accuracy of the proposed method is superior to that of the literature [22] and [14].

C. *Robustness Analysis and Comparison*

The purpose of the experiment in this section is to test whether the proposed method is robust to incidental changes caused by image post-processing operations. In the experiment, we selected 180 images from Columbia IPDED database. In order to quantitatively analyze the robustness of the proposed method, we performed some post-processing operations on these tested images, and compare the detection results of the proposed method with literature [22] and [14], respectively. Then we calculate the mean values of pixel level *TPR* and *FPR* of all tested images. The experimental results are shown in Table 2.

Table 2 Comparison of robustness performance

	The proposed method		[22]		[14]	
	TPR	FPR	TPR	FPR	TPR	FPR
NO post-processing	71.8	9.7	67.3	38.1	47.9	18.5
JPEG compression	60.5	11.3	64.5	40.4	22.0	10.8
Down-sampling	67.8	12.5	60.3	39.8	46.0	23.5
Gamma correction	62.7	11.7	62.4	37.6	31.9	17.4
Gaussian blur	61.4	10.2	61.5	40.2	33.3	19.7

IV. CONCLUSION

In this paper, we propose an image splicing localization method based on inconsistent noise levels. In the proposed method, we use Laplace noise and prediction error noise as the forensics features, and use the FCM clustering algorithm and the adaptive threshold to locate the spliced image regions. Compared with existing methods, the proposed method is provided with satisfactory splicing localization accuracy, and has better robustness against post-processing operations.

REFERENCES

[1] M. Holliman, N. Memon, "Counterfeiting attacks on oblivious block-wise independent invisible watermarking schemes," IEEE Transactions on Image Processing, vol. 9, no. 3, pp. 432-441, 2000.

[2] H. H. Tsai, C. C. Liu, "Wavelet-based image watermarking with visibility range estimation based on HVS and neural networks," Pattern Recognition, vol. 44, no. 4, pp. 751-763, 2011.

[3] U. H. Panchal, R. Srivastava, "A Comprehensive Survey on Digital Image Watermarking Techniques," Fifth International Conference on Communication Systems and Network Technologies, pp. 591-595, 2015.

[4] B. Mahdian, S. Saic, "A bibliography on blind methods for identifying image forgery," Signal Processing: Image Communication, vol. 25, no. 6, pp. 389-399, 2010.

[5] G. K. Birajdar, V. H. Mankar, "Digital image forgery detection using passive techniques: A survey," Digital Investigation, vol. 10, no. 3, pp. 226-245, 2013.

[6] X. Wang, G. He, C. Tang, "Keypoints-Based Image Passive Forensics Method for Copy-Move Attacks," International Journal of Pattern Recognition and Artificial Intelligence, vol. 30, no. 3, pp. 23, 2016.

[7] Z. He, W. Lu, W. Sun, "Digital image splicing detection based on Markov features in DCT and DWT domain," Pattern Recognition, vol. 45, no. 12, pp. 4292-4299, 2012.

[8] W. Zhang, X. Tang, Z. Yang, "Multi-scale segmentation strategies in PRNU-based image tampering localization," Multimedia Tools and Applications, vol. 78, no. 14, pp. 1-20, 2019.

[9] B. Wang, X. Kong, "Image splicing localization based on re-demosaicing," Advances in Information Technology and Industry Applications. Springer, Berlin, Heidelberg, vol. 136, pp. 725-732, 2012.

[10] F. Xue, W. Lu, Z. Ye, "JPEG image tampering localization based on normalized gray level co-occurrence matrix," Multimedia Tools and Applications, vol. 78, no. 8, pp. 9895-9918, 2019.

[11] K. Bahrami, A. C. Kot, L. Li, "Blurred image splicing localization by exposing blur type inconsistency," IEEE Transactions on Information Forensics and Security, vol. 10, no. 5, pp. 999-1009, 2015.

[12] B. Mahdian, S. Saic, "Using noise inconsistencies for blind image forensics," Image and Vision Computing, vol. 27, no. 10, pp. 1497-1503, 2009.

[13] D. L. Donoho, J. M. Johnstone, "Ideal spatial adaptation by wavelet shrinkage," biometrika, vol. 83, no. 3, pp. 425-455, 1994.

[14] H. Zeng, Y. Zhan, X. Kang, "Image splicing localization using PCA-based noise level estimation," Multimedia Tools and Applications, vol. 76, no. 4, pp. 4783-4799, 2017.

[15] T. Julliand, V. Nozick, H. Talbot, "Automated image splicing detection from noise estimation in raw images," Sixth International Conference on Imaging for Crime Prevention and Detection, pp. 6-13, 2015.

[16] C. M. Pun, B. Liu, X. C. Yuan, "Multi-scale noise estimation for image splicing forgery detection," Journal of visual communication and image representation, vol. 38, pp. 195-206, 2016.

[17] O. Veksler, Y. Boykov, P. Mehrani, "Superpixels and supervoxels in an energy optimization framework," In European conference on Computer vision. Springer, Berlin, Heidelberg, vol. 6315, pp. 211-224, 2010.

[18] J. Immerkaer, "Fast noise variance estimation," Computer vision and image understanding, vol. 64, no. 2, pp. 300-302, 1996.

[19] Z. P. Zhou, X. X. Zhang, "Image splicing detection based on image quality and analysis of variance," Second International Conference on Education Technology and Computer, vol. 4, pp. 4-242, 2010.

[20] N. R. Pal, J. C. Bezdek, "On cluster validity for the fuzzy c-means model," IEEE Transactions on Fuzzy Systems, vol. 3, no. 3, pp. 370-379, 1995.

[21] N. Otsu, "A threshold selection method from gray-level histograms," IEEE transactions on systems, man, and cybernetics, vol. 9, no. 1, pp. 62-66, 1979.

[22] N, Zhu, Z, Li, "Blind image splicing detection via noise level function," Signal Processing: Image Communication, vol. 68, pp. 181-192, 2018.

[23] T. T. Ng, J. Hsu, S. F. Chang, "Columbia image splicing detection evaluation dataset", 2009.